ORIGINAL PAPER

Estimation of psychomotor delay from the Fitts' law coefficients

**Dan Beamish · Shabana Bhatti · C. Scott Chubbs ·
I. Scott MacKenzie · Jianhong Wu · Zhujun Jing**

Abstract An intrinsic property of human motor behavior is a trade-off between speed and accuracy. This is classically described by Fitts' law, a model derived by assuming that the human body has a limited capacity to transmit information in organizing motor behavior. However, Fitts' law can also be realized as an emergent property of movements generated by delayed feedback. In this article, we describe the relationship between the Fitts' law coefficients and the physiological parameters of the underlying delayed feedback circuit: the relaxation rate or time constant, and the psychomotor delay of the feedback process. This relationship is then used to estimate the motor circuit delay of several tasks for which Fitts' law data are available in the literature. We consistently estimate the delay to be between 0 and 112 ms. A further consequence of this model is that not all combinations of slope and Y-intercept in Fitts' law are possible when movements are generated by delayed feedback. In fact, it is only possible for an observed speed–accuracy trade-off to be generated by delayed feedback if the Fitts' law coefficients satisfy $-0.482 \leq a/b \leq 3.343$ [bits] where b represents the slope in bits per second and a represents the Y-intercept in seconds. If we assume human movement is generated by delayed feedback, then the Fitts' law coefficients should always be restricted to this range of values.

Keywords Fitts' law · Psychomotor delay ·
Motor performance · Motor control · Neurodynamics

D. Beamish (✉) · Z. Jing
Chinese Academy of Science, Academy of Mathematics
and Systems Science, Beijing, China
e-mail: dan.beamish@gmail.com

S. Bhatti
Department of Biology, York University, Toronto, Canada

C. S. Chubbs
University of Ottawa Medical School, Ottawa, Canada

I. S. MacKenzie
Department of Computer Science and Engineering,
York University, Toronto, Canada

J. Wu
Laboratory for Industrial and Applied Mathematics,
York University, Toronto, Canada

1 Introduction

An intrinsic property of the human motor behavior is a trade-off between speed and accuracy (Woodworth 1899). This is classically described by Fitts' law (1954), a model derived by assuming that the human body has a limited capacity to transmit information in organizing motor behavior. Within this model, the time to perform a task is proportional to the amount of information (in bits) required on average for producing the movement. This quantity is known as the Index of Difficulty (ID) of a task and is often quantified using the Shannon Coding Theorem with movement time (MT) given as

$$\text{MT} = b \cdot \text{ID} = b \cdot \log_2 \left(\frac{A}{W} + 1 \right),$$

where A is the amplitude of the movement, W is the tolerance or target width (MacKenzie 1989), and the slope b is determined empirically. The inverse of the slope $1/b$, which has units of bits per second, is interpreted as the information capacity of the motor "channel" used in performing the task. Experimentally, where a model is built using

linear regression, Fitts' law usually appears as

$$\text{MT} = a + b \cdot \text{ID} = a + b \log_2\left(\frac{A}{W} + 1\right),$$

with both the slope b and Y-intercept a as measured values.

In the more than 50 years since originally described, there have been many investigations into what physiological processes occur during movement that give rise to Fitts' law beyond the information hypothesis. Furthermore, Fitts' law is so universally observed that any model of human motor control must account for its predictions. One modeling approach is that Fitts' law arises as an emergent property of delayed feedback control within the motor circuit (Gawthrop et al. 2007; Beamish et al. 2006; Connelly 1984; Cannon 1994; Phillips and Repperger 1997; Jagacinski and Flach 2003). Because signals are not transmitted instantaneously through the human body, movement taking place on time scales smaller than the required delay could not have sensory or other feedback information available to coordinate or control the movement. This naturally gives rise to a speed–accuracy trade-off since the accuracy of faster movements is diminished by the larger distances being moved during the time required for those signals to be received.

There is strong neurobiological evidence in support of feedback determining motor performance: The Vector Integration To Endpoint (VITE) circuit (Bullock and Grossberg 1988) is one of the earliest models to suggest that invariant properties of movement such as Fitts' law are best understood as emergent properties of underlying neurobiological mechanisms. Within the VITE model, inequalities of distance are translated into neural commands as differences in the amount of contraction by muscles forming a synergy (Hollerback et al. 1986). Motor planning occurs in the form of a Target Position Command (TCP) which specifies the desired target position, and an independently controlled gain signal (G) regulating the overall movement speed. Automatic feedback processes between nerve populations of the motor circuit then convert these signals into a movement trajectory. This includes a Present Position Command (PPC) specifying an internal representation of the current position, and a Difference Vector (DV) command specifying the difference between the present and target position at any given time. The PPC generates a pattern of outflow movement signals to muscle groups causing movement toward the target, and is gradually updated by integrating signals from the DV through time. The DV signals are multiplied by the gain signal prior to integration, which serves to regulate the movement speed. Throughout the movement, the PPC additionally sends signals back to the DV population which aid in the computation of the difference vector. See Fig. 1 which contains a network diagram of the VITE circuit.

Movement trajectories are generated by negative feedback as outflow motor commands from the PPC cause movement

Fig. 1 A network diagram of the VITE circuit with connections indicated as excitatory or inhibitory. *TPC* target position command, *PPC* present position command, *DV* difference vector, *G* gain signal
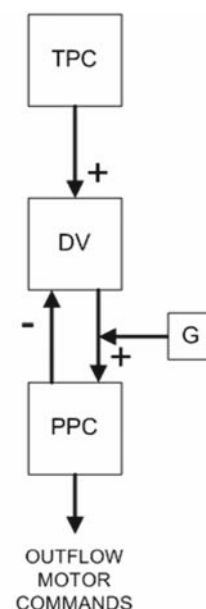
toward the target, in turn, causing the DV to be reduced. This feedback suffers from two separate delays: the delay in response of the muscle plant to outflow motor commands by the PPC; and the delay with which the DV population responds to the signals sent back from the PPC giving present position information. It is highly likely that a forward predictor mechanism operates at this stage, the purpose of which is to compensate for delay by anticipating the response of the muscles and environment to outflow motor commands (Miall and Wolpert 1996; Tunik et al. 2005; Cisek 2001).

The simplest model consistent with the above constraints obeys the set of nonlinear delay differential equations

$$\frac{\mathrm{d}V}{\mathrm{d}t} = \alpha \left[-V(t) + T(t) - P(t - \tau_1) \right], \tag{1}$$

$$\frac{\mathrm{d}P}{\mathrm{d}t} = G \cdot [V(t - \tau_2)]^+, \tag{2}$$

where $T(t)$ and $P(t)$ represent the PPC and TPC activities, $V(t)$ represents the DV population activity, G represents the gain signal, and where

$$[V(t)]^+ = \begin{cases} 0 & \text{if } V(t) \leq 0 \\ V(t) & \text{if } V(t) > 0 \end{cases}.$$

The first equation says that the activity of the DV population averages the difference between the target and position command signal by bringing $V(t)$ toward the equilibrium value of $V(t) = T(t) - P(t)$ with rate or time constant, α, but having a delayed response time, τ_1, to present position signals. The larger the value of α, which has units of 1/ms, the more quickly the DV population adapts to the changing present position command. The second equation asserts that the PPC cumulatively integrates the DV signals multiplied by the gain, G, and delayed by the time, τ_2, required for response to outflow motor commands—but only for such a

duration as the DV generates a positive signal from the presence of the cutoff function. The cutoff function appearing in Eq. 2 allows only unidirectional movement toward the target by halting the dynamics once the DV population becomes zero. It is a deceptively simple nonlinearity that introduces an infinite number of equilibria to the delay dynamical system (1–2) and prevents the application of standard analytical techniques for dynamical systems. See Beamish et al. (2005) and Beamish et al. (2006) for a discussion of the VITE circuit dynamics.

A tacit assumption made by the system (1–2) is that the limb response to outflow signal size is linear. Muscle plant characteristics can change through time because of growth and development, aging, exercise, transient changes in blood supply, or minor tears. Therefore, it is not known a priori how much a muscle will contract in response to an outflow signal of a prescribed size, or how the limb will move in response to a prescribed muscle synergy contraction. Bullock and Grossberg propose that auxilliary circuits serve to adaptively modify outflow motor commands to produce a linear correspondence between the signal size and amount of contraction even if the muscle plant is nonlinear. See Bullock and Grossberg (1988) for a discussion. This mechanism of adaptive linearization has obvious similarities to the forward predictor mentioned above although it is not clear if they are the same.

An interesting and remarkable property of the VITE circuit is that it possesses a speed–accuracy trade-off consistent with Fitts' law and potentially explaining many experimental inconsistencies of the information model (Beamish et al. 2006). The ideal circuit operating with no delays has a performance identical with the predictions of the information hypothesis so that $MT = b \cdot ID$ (Bullock and Grossberg 1988). When delay is activated, however, the Y-intercept becomes non-zero and may even be negative so that $MT = a + b \cdot ID$. Negative Y-intercepts have been problematic since, to be consistent with the information hypothesis, the intercept should be $(0, 0)$ predicting 0 ms to complete a task requiring 0 bits. For this reason, the intercept is often regarded as an "error" term in most of the literature on Fitts' law (e.g., Soukoreff and MacKenzie 2004). Several interpretations of a non-zero Y-intercept have been described, including: unavoidable delay in the psychomotor system (Fitts and Radford 1966); uncontrollable muscle activity at the beginning or end of the movement task (MacKenzie 1992); and reaction time (Fitts 1964). However, these explanations are compromised because negative intercepts often occur, and they are frequently too large to be attributed to random variations in subject performance (Soukoreff and MacKenzie 2004).

In this article, we describe the relationship between the coefficients occurring in Fitts' law and the physiological parameters of the VITE circuit: the feedback time constant or relaxation rate; and the psychomotor delay. This relationship is then used to estimate the motor pathway delay of several tasks for which Fitts' law data are available in the literature. We consistently estimate values between 0 and 112 ms with the majority found to be less than 60 ms. However, it is not clear what specific neural pathway this delay might actually correspond to. Furthermore, if a forward predictor mechanism operates to compensate for the motor circuit delay, then what we actually estimate would be the *effective* total delay of the feedback process giving rise to the observed speed–accuracy trade-off instead of nerve conduction time. If this is the case, present position information derived during the performance of different tasks may rely on specific task-dependent neural mechanisms with different effective delays, complicating the interpretation of any estimate.

An additional property of the VITE circuit is that there exists a maximum performance possible when delay is present (Beamish et al. 2008). This is strictly a delay effect and is a completely different behavior from the classical Fitts' law as a regression model where slope and Y-intercept may take arbitrary values. Here, we show that, as an unexpected consequence of this performance limit, it is only possible for an observed speed–accuracy trade-off to have been generated by the delayed feedback process of the VITE circuit if the Fitts' law coefficients satisfy $-0.482 \leq a/b \leq 3.343$ bits. Assuming that the VITE circuit is a satisfactory model of human motor control we should always expect the Fitts' law coefficients to be restricted to this range. A survey of various Fitts' law data sets reported in the literature finds this to be the case with the few exceptions explainable by methodological problems in the motor experiment design. Moreover, this should be an ubiquitous property of any delayed linear feedback controller that is only capable of unidirectional movement.

The outline of this article is as follows. Section 2 describes the speed–accuracy performance of the delayed VITE circuit. Section 3 describes the explicit relationship between the VITE circuit parameters and the Fitts' law coefficients. Here, it is also demonstrated that under the assumptions of the VITE model the Fitts' law coefficients always satisfy the restriction mentioned above. Section 4 gives an analysis of various Fitts' law data sets available in the literature to estimate the motor circuit parameters, in particular, the psychomotor delay, and to support the finding that the Fitts' law coefficients are, in fact, restricted. Section 5 concludes the article with a discussion and interpretation of the results.

2 The performance of the VITE circuit

When considering the dynamics of the VITE circuit, we assume throughout this article that it is initially in an equilibrium state where PPC and TPC are equal. At time zero,

a new target position stimulus is presented causing movement toward the target as the PPC shifts toward the new equilibrium. It is not difficult to show through a change of variables that the dynamics of the circuit depends only on the total amount of delay $\tau = \tau_1 + \tau_2$. For the circuit with fixed parameters, α, τ, the qualitative behavior of the PPC trajectory depends only on the magnitude of the gain signal, G: if the gain is sufficiently large, then the PPC overshoots the target and comes to rest after a finite time; otherwise, the PPC asymptotically approaches the target without overshooting (Theorem 1 from Beamish et al. 2005). Once the target and gain signals have been specified, the movement time and amount of target overshoot are determined automatically by negative feedback between the PPC and DV populations. We may, therefore, formulate a speed–accuracy trade-off for the circuit by considering the question: *What is the minimum movement time required after initial presentation of a fixed target stimulus to move through an amplitude A and come to rest within a target zone of width W?* It can further be shown that movement times are independent of the amplitude, A, and the amount of target overshoot is proportional to the movement amplitude so that the minimum movement time required may be considered to be a function of A/W or, alternatively, as a function of the Index of Difficulty, $\text{ID} = \log_2\left(\frac{A}{W} + 1\right)$ (Theorems 3 and 6 from Beamish et al. 2006, respectively).

There is flexibility here in how we choose to define "movement time" of a trajectory that will later affect our estimation of psychomotor delay from the speed–accuracy trade-off observed for a motor task. For example, should the measurement of movement time begin at the time when the initial target stimulus is presented (as might be measured during a reciprocal tapping task), or, at the time when movement toward the target begins (as might be measured with a discrete task)? The difference in time between these two definitions would be exactly $\tau_1 + \tau_2$: the delay between target stimulus presentation and movement toward the target. In addition, we could also consider the time required for the PPC to enter the target zone, instead of the time at which the PPC reaches equilibrium and comes to rest, although we do not consider that in this article. We state the following definitions of movement time for clarity:

Definition 1 (*Stimulus-based*) The movement time $\text{MT}_{\alpha,\tau}^{\text{Stimulus}}(\text{ID})$ of a VITE circuit trajectory is the minimum time measured from the initial target stimulus presentation required to move through a distance A and come to rest within a distance W of the target (Remember that this depends only on A/W and is, therefore, a function of ID.).

Definition 2 (*Movement-based*) The movement time $\text{MT}_{\alpha,\tau}^{\text{Movement}}(\text{ID})$ of a VITE circuit trajectory is the minimum time measured from the beginning of movement after the initial target stimulus presentation required to move through

a distance A and come to rest within a distance W of the target.

Also, as remarked above, we have

$$\text{MT}_{\alpha,\tau}^{\text{Stimulus}}(\text{ID}) = \tau + \text{MT}_{\alpha,\tau}^{\text{Movement}}(\text{ID}).$$

Unless otherwise specified, movement time $\text{MT}_{\alpha,\tau}(\text{ID})$ will refer to the stimulus-based definition $\text{MT}_{\alpha,\tau}^{\text{Stimulus}}(\text{ID})$. We refer to the speed–accuracy trade-off between movement time and ID as simply the "performance" of the circuit for a given pair of parameters α, τ.

When the delay is zero, the Eqs. 1 and 2 can be solved exactly and the speed–accuracy trade-off is

$$\text{MT} = \frac{2\ln 2}{\alpha} \log_2\left(\frac{A}{W}\right),$$

a straight line through the origin consistent with the information-theoretic paradigm (Appendix A from Bullock and Grossberg 1988). When delay is activated, an approximately linear relationship with non-zero Y-intercept continues to hold for movement times that are large relative to the delay so that $\text{MT}_{\alpha,\tau}(\text{ID}) \approx a + b \cdot \text{ID}$, but as the ID diminishes a nonlinear breakdown occurs in which the predicted movement time approaches the lower limit of 2τ imposed by delay (Beamish et al. 2006). The Y-intercept a may be either positive or negative, with both the Y-intercept a and slope b nonlinearly coupled to both the delay τ, and the DV population relaxation rate, α. There is no simple expression for this relationship although it is computable by integration of the model equations as described below. It is this relationship between the Fitts' law coefficients, a, b, and the physiological relaxation rate, α, and psychomotor delay, τ, that is considered in the following sections.

2.1 Method

Our method of computing the performance of the VITE circuit is based on the following result that for any constant, $c > 0$, we have

$$c \cdot \text{MT}_{\alpha,\tau}(\text{ID}) = \text{MT}_{\frac{\alpha}{c}, c\tau}(\text{ID}). \tag{3}$$

In other words, scaling the movement times by c gives the speed–accuracy trade-off corresponding to the circuit having delay multiplied by c and the DV population relaxation rate, α, multiplied by $\frac{1}{c}$. This is found simply by rescaling time in the model Eqs. 1–2 (see Theorem 11 from Beamish et al. 2008). The advantage of this is that we can determine the performance of the circuit with arbitrary parameters after we know the performances of the circuit having either $\alpha = 1$ or $\tau = 1$. This will be important later for both estimating delay from measured movement times and showing there is only a limited range of possible slope and intercept values possible for the speed–accuracy trade-off of the VITE circuit:

Theorem 1 *The performance for the circuit with parameters a, τ are determined from the performance of the circuit with either $\alpha = 1$ or $\tau = 1$ using*

$$\mathrm{MT}_{\alpha,\tau}(\mathrm{ID}) = \frac{1}{\alpha} \cdot \mathrm{MT}_{1,\alpha\tau}(\mathrm{ID}) = \tau \cdot \mathrm{MT}_{\alpha\tau,1}(\mathrm{ID}). \qquad (4)$$

Proof Substituting $c = \alpha$ into Eq. 3 above and dividing both sides by α, we have the result for $\alpha = 1$. Substituting $c = 1/\tau$ and multiplying both sides by τ gives the other.

The performance curves were calculated by integrating the model Eqs. 1 and 2 using the dde23 routine of Matlab v7.5 to obtain the amount of target overshoot and movement time for different values of gain G. This gives individual points (ID,MT) along the performance curve. A sufficient number of points are calculated so that there is at least one within each 0.2 bit interval between 0 and 10 bits. We then use linear interpolation to determine the values of $\mathrm{MT}_{\alpha,\tau}(\mathrm{ID})$ at intermediate points throughout the interval. The Matlab code is included in the supplemental material for this article.

3 The relationship between the model parameters and the Fitts' law coefficients

In Beamish et al. (2008) it is shown that the VITE circuit is not capable of arbitrarily high performance movements when delay is present. Here, we show that, as a consequence of this performance limit, not all values for the Fitts' law slope and intercept coefficients have corresponding VITE circuit parameters, α, τ, giving rise to that speed–accuracy trade-off. In fact, only when the coefficients satisfy $-0.482 \leq a/b \leq 3.343$ [bits] do there exist corresponding values of α, τ such that $\mathrm{MT}_{\alpha,\tau}(\mathrm{ID}) \approx a + b \cdot \mathrm{ID}$. We describe the general relationship between the VITE circuit parameters and the Fitts' law coefficients when they do exist. This will be used in the next section to estimate psychomotor delay from speed–accuracy trade-off reported in the literature for various motor tasks.

Toward this goal, it is convenient to consider the circuit in terms of two new parameters $c = 1/\alpha$ and $k = \alpha\tau$ so that, using Eq. 3 above, we have

$$c \cdot \mathrm{MT}_{1,k}(\mathrm{ID}) = \mathrm{MT}_{1/c,ck}(\mathrm{ID}) = \mathrm{MT}_{\alpha,\tau}(\mathrm{ID}). \qquad (5)$$

This is done without loss of generality and has the advantage that now the speed–accuracy trade-off $c \cdot \mathrm{MT}_{1,k}(\mathrm{ID})$ is linear in the variable c. The variable, $k = \alpha\tau$, the product of the time constant and the delay, determines the "shape" of the speed–accuracy trade-off (always approximately a straight line with nonlinear breakdown as the movement time approaches the delay). After we know the relationship between the slope and intercept of $\mathrm{MT}_{1,k}(\mathrm{ID})$ for the different values of k (i.e., the performance of the circuit with time

constant $\alpha = 1$ for different delays), it is easy to determine the rest because the dependence on c is simply linear.

Suppose that the speed–accuracy trade-off $\mathrm{MT}_{1,k}(\mathrm{ID})$ is approximately linear so that

$$\mathrm{MT}_{1,k}(\mathrm{ID}) \approx a(k) + b(k) \cdot \mathrm{ID} \qquad (6)$$

where the slope $b(k)$ and Y-intercept $a(k)$ depends on k. We may normalize the slope to 1 if we choose $c = 1/b(k)$ so that

$$\frac{1}{b(k)}\mathrm{MT}_{1,k}(\mathrm{ID}) \approx \frac{a(k)}{b(k)} + \mathrm{ID}, \qquad (7)$$

and the Y-intercept becomes $a(k)/b(k)$. Furthermore, for each $k > 0$, there is only one value of c that would make the slope equal to 1 because of the linear dependence. Multiplying Eq. 7 by a positive constant b' gives a new parameter $c = b'\frac{1}{b(k)}$ for which

$$b'\frac{1}{b(k)}\mathrm{MT}_{1,k}(\mathrm{ID}) \approx b'\frac{a(k)}{b(k)} + b' \cdot \mathrm{ID}, \qquad (8)$$

so that the slope becomes b' and the Y-intercept becomes $b'\frac{a(k)}{b(k)}$.

Now, although we can always choose the parameter, (c, k), to make the slope, b' of any value we want, the Y-intercept must always be $b'\frac{a(k)}{b(k)}$, which is dependant on both the slope and the ratio $a(k)/b(k)$. If this ratio takes all possible real values $(-\infty, \infty)$, then we could also make the Y-intercept of any value we want by choosing appropriate values of k and c. However, this is not the case. Instead, it takes on only a finite range of values due to the limiting behavior of the circuit as $k \to 0$ or $k \to \infty$:

(i) In the limit as $k \to 0$, the performance of the circuit approaches that of the ideal circuit with zero delay so that

$$\mathrm{MT}_{1,k}(\mathrm{ID}) = 2\ln 2 \log_2\left(\frac{A}{W}\right).$$

(ii) In the limit as $k \to \infty$, the performance of the circuit approaches its maximum limit described by Eq. 17 in Beamish et al. (2008) so that

$$\mathrm{MT}_{1,k}(\mathrm{ID}) \approx k\,(0.049 + 0.687 \cdot \mathrm{ID}).$$

Note that the slope and intercept occurring in this upper limit change slightly depending on how we choose to make the linear approximation in Eq. 6.
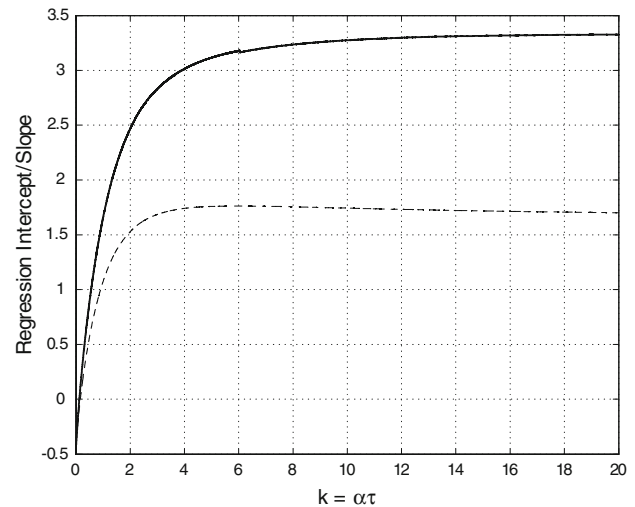
The effect that this limiting behavior has on the range of possible Y-intercept values may be seen in Fig. 2 which contains graphs of $\mathrm{MT}_{1,k}(\mathrm{ID})$ for which the slope has been normalized to 1 for various values of k. The Y-intercepts are equal to the ratio, $a(k)/b(k)$, which is clearly seen to take
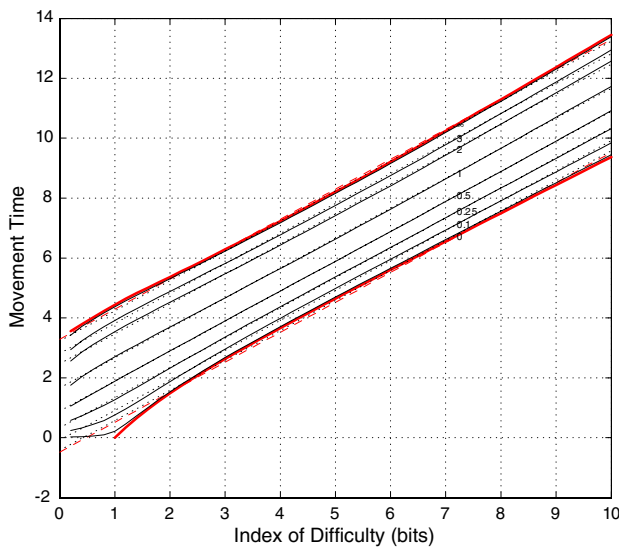
Fig. 2 Performance curves $MT_{1,k}(ID)$ are normalized so that the linear regression has a slope of 1 (*solid*) and the regression line (*dotted*) for $k = \alpha\tau$ of 0, 0.01, 0.1, 0.25, 0.5, 1, 2, 3, 10, and ∞. Observe that these curves approach a limit as $k \to 0$ or $k \to \infty$. The normalized performance curves as $k = \alpha\tau \to 0, \infty$ are shown in *red*. The only possible performance curves for the delayed feedback circuit are the constant multiples of these, and thus only take on a finite range of slope and intercept values (color figure online)

Fig. 3 Graph of the intercept divided by slope for linear regression of the performance curve $MT_{1,k}(ID)$ as a function of k. The *solid line* uses the stimulus-based definition of MT while the *broken line* uses the movement-based definition. Regression curves are computed by sampling the performance curve at intervals of 0.2 bits between 1 and 10 bits

only a finite range of values. Figure 3 contains graphs of this Y-intercept as a function of k using the two different definitions of movement time. We find that $-0.482 \leq a(k)/b(k) \leq 3.343$ for the stimulus-based definition of movement time, and $-0.478 \leq a(k)/b(k) \leq 1.763$ for the movement-based definition. Keep in mind that the exact values of the slope $b(k)$ and Y-intercept $a(k)$ are dependent on how we choose to make the linear approximation in Eq. 6. The method used throughout this article is by sampling the speed–accuracy trade-off MT(ID) at evenly spaced points 0.2 bits apart between 1 and 10 bits and, then, performing linear regression to determine the slope and intercept coefficients. We ignore the region between 0 and 1 bit because this is where the highest amount of nonlinearity occurs in the relationship MT(ID) and is the hardest region to experimentally measure movement time, although variations on this do not seem to greatly affect the end result. From the above analysis, there exist values of the VITE circuit parameters α, τ corresponding to the Fitts' law coefficients $MT = a + b \cdot ID$, if and only if, $-0.482 \leq a/b \leq 3.343$.

The argument above has the further advantage of giving us the relationship between the VITE model parameters α, τ and the Fitts' law coefficients a, b. After the slope and Y-intercept have been determined for $MT_{1,k}(ID)$ as in Eq. 6, Eq. 7 gives us the relationship between the model parameters c, k (and hence α, τ) and the Y-intercept $a(k)/b(k)$ when the slope is equal to one. This is displayed in Fig. 4. The parameters for

any values of slope and intercept can then be determined by first normalizing the slope to 1 as in Eq. 7—i.e., by dividing the intercept by the slope—and then looking up the resulting value of k corresponding to the new Y-intercept as above.

Figures 5 and 6 contain the complete relationship between the Fitts' law coefficients and the model parameters using the stimulus-based definition of movement time computed using the approach described above. Figures 7 and 8 contain this relationship using the movement-based definition of movement time. The estimated relationship is clearly seen to be different between the two definitions so that any estimate of delay is highly sensitive to considerations of reciprocal versus discrete experimental design (among other factors).

## 4 Estimation of psychomotor delay from the observed speed–accuracy trade-off

In the previous section, we considered the relationship between the model parameters of the VITE circuit and the Fitts' law coefficients. Here, we use this relationship to estimate the psychomotor delay involved in various tasks for which the speed–accuracy trade-off is reported in the literature. Specifically, we consider the collection of data sets presented in the appendices of MacKenzie (1991). These include Fitts' reciprocal tapping, pin and disc transfer tasks; computer input tasks; and 25 additional data sets from various studies.

For a given set of experimentally measured movement times (ID_i, MT_i), a nonlinear regression was used to determine the model parameters α, τ which minimize the least-squares difference
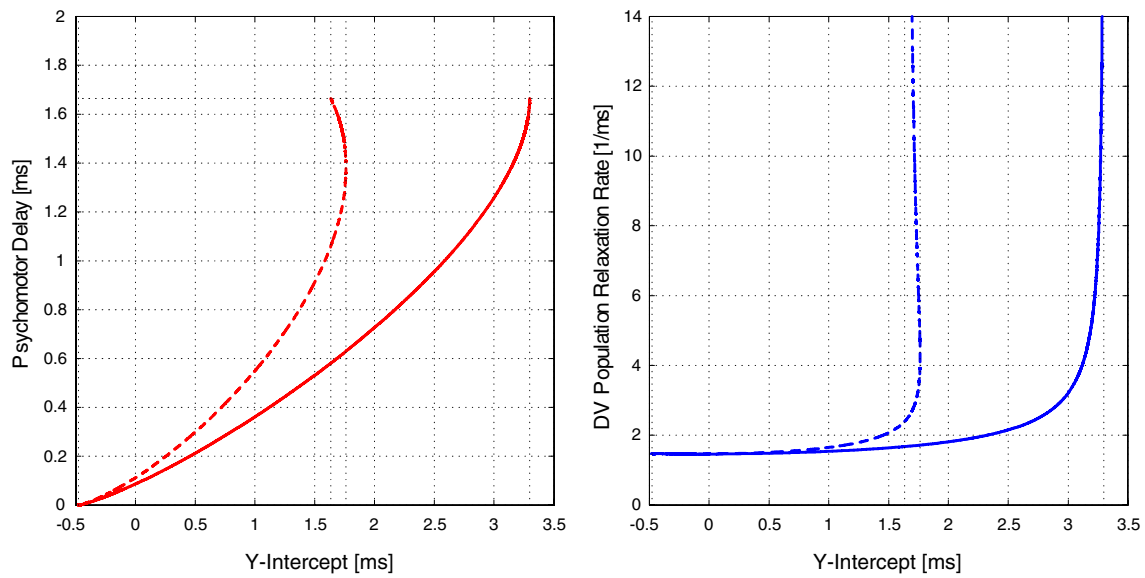
Fig. 4 Model parameters α (*blue*) and τ (*red*) as a function of the intercept when slope equals 1. The values of each parameter are dependent on the definition of movement time: stimulus-based (*solid line*) or movement-based (*broken line*). Note that for the movement-based definition the parameters are nonunique and appear to consist of two branches near the upper limits of the intercept (color figure online)
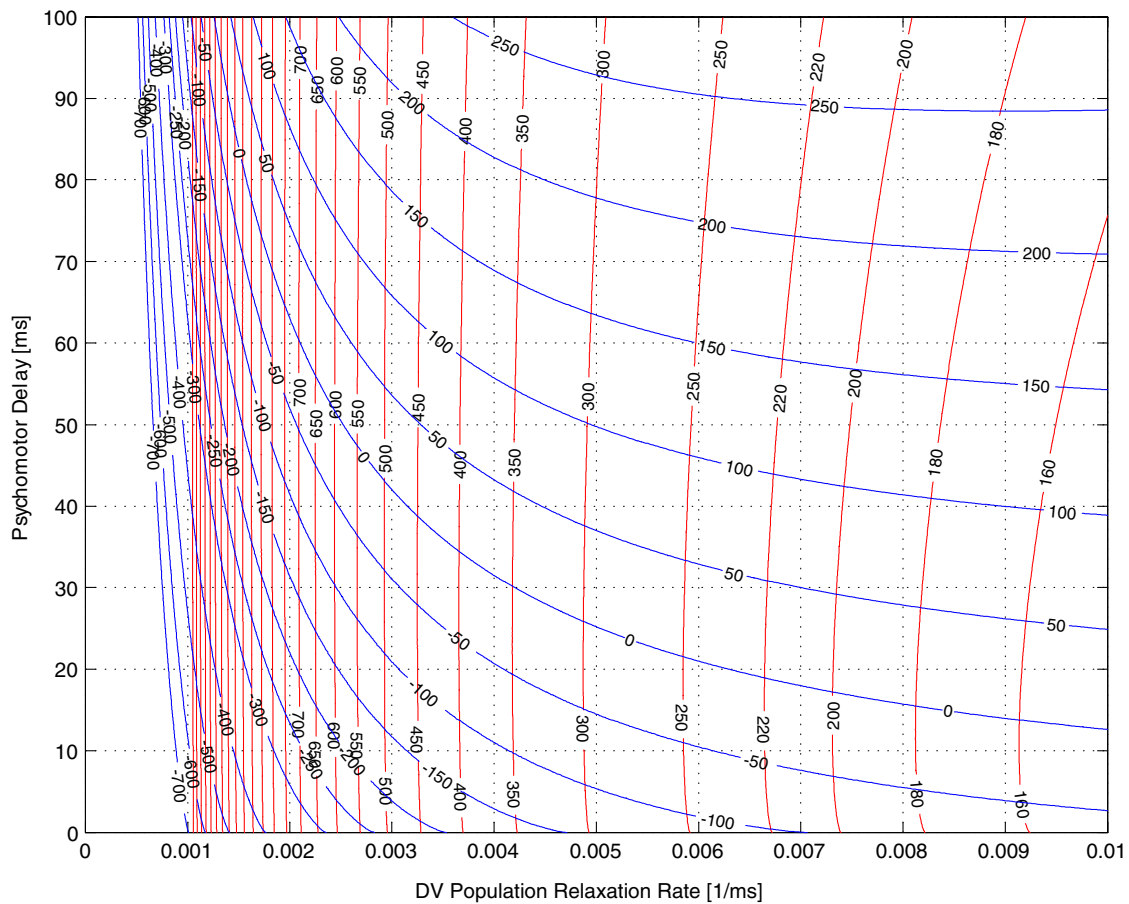
Fig. 5 Contour diagram of the Fitts' law slope (*red*) and *Y*-intercept (*blue*) dependence on the model parameters using the stimulus-based definition of MT. Linear regression was performed at evenly spaced points 0.2 bits apart between 1 and 10 bits (color figure online)
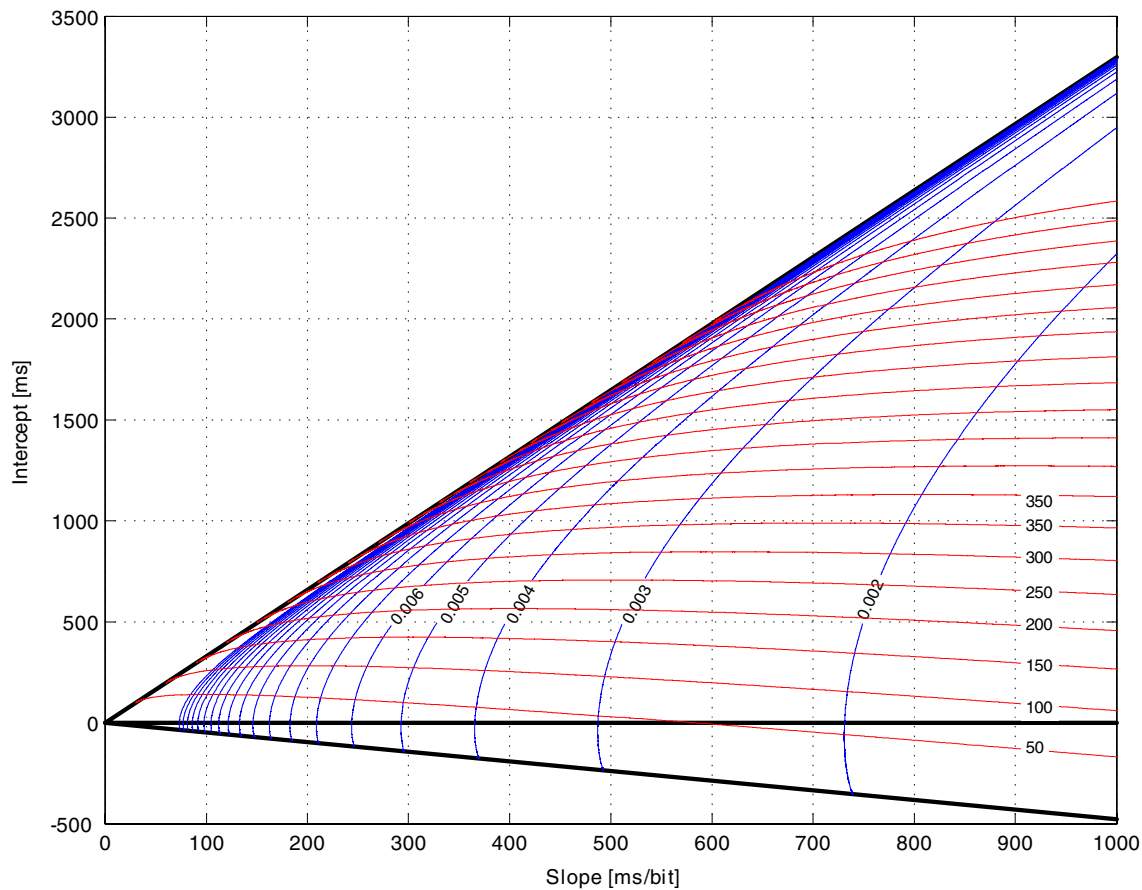
Fig. 6 Contour diagram of the relationship between the Fitts' law slope and Y-intercept, and the model parameters, delay τ (*red*) and DV population relaxation rate α (*blue*) using the stimulus-based definition of movement time. Contours for delay are every 50 ms. Contours for relaxation rate are every 0.001 ms/bit. Linear regression was performed at evenly spaced points 0.2 bits apart between 1 and 10 bits (color figure online)

$$\Delta(\alpha, \tau) = \sqrt{\sum_{i=1}^{n} \left(\mathrm{MT}_{\alpha,\tau}(\mathrm{ID}_i) - \mathrm{MT}_i \right)^2}$$

between the experimental data and the speed–accuracy trade-off of the delayed feedback circuit. This allows for the possibility that the natural nonlinearity of the delayed feedback circuit performance might have a superior or inferior fit to the measured data compared with linear regression. The definition of movement time used here will affect the estimation of the parameters and, ideally, should be identified with what has been measured. However, we assume throughout this section that movement time begins when the initial stimulus is presented.

It is convenient to use Eq. 5 to express the speed–accuracy trade-off of the VITE model in terms of the variables c, k so that

$$\Delta(c, k) = \sqrt{\sum_{i=1}^{n} \left(c \cdot \mathrm{MT}_{1,k}(\mathrm{ID}_i) - \mathrm{MT}_i \right)^2}$$

which now has a linear dependence on the variable c. It is also necessary to consider only a finite range for the variable

k because of the limiting behavior mentioned in the previous section as k becomes large. By precomputing $\mathrm{MT}_{1,k}(\mathrm{ID})$ and using these simplifications, it is straightforward to calculate $\Delta(\alpha, \tau)$ and find the global minimum. These are reported in Table 1.

In order to estimate a range for the delay, a contour plot is created showing those parameter values (α, τ) for which the difference between the model and the data is within 10% of the difference between the linear regression and the data. Figure 9 contains graphs of the estimated parameters for the unadjusted data of the six computer input tasks presented in Appendix B of MacKenzie (1991). Estimates for psycho-motor delay for these tasks are found to be between 16 and 109 ms. Figure 10 contains graphs of the estimated parameters for Fitts' original 1954 reciprocal tapping, pin, and disc transfer tasks. The data provided for the reciprocal tapping tasks allow re-analysis to include adjustment for accuracy that will be discussed below. The estimated delay and relaxation rate for the remaining data sets are contained in Fig. 11 while Fig. 12 contains graphs comparing the speed–accuracy trade-off of the delayed feedback model with the linear regression. The estimated delays for all the motor tasks
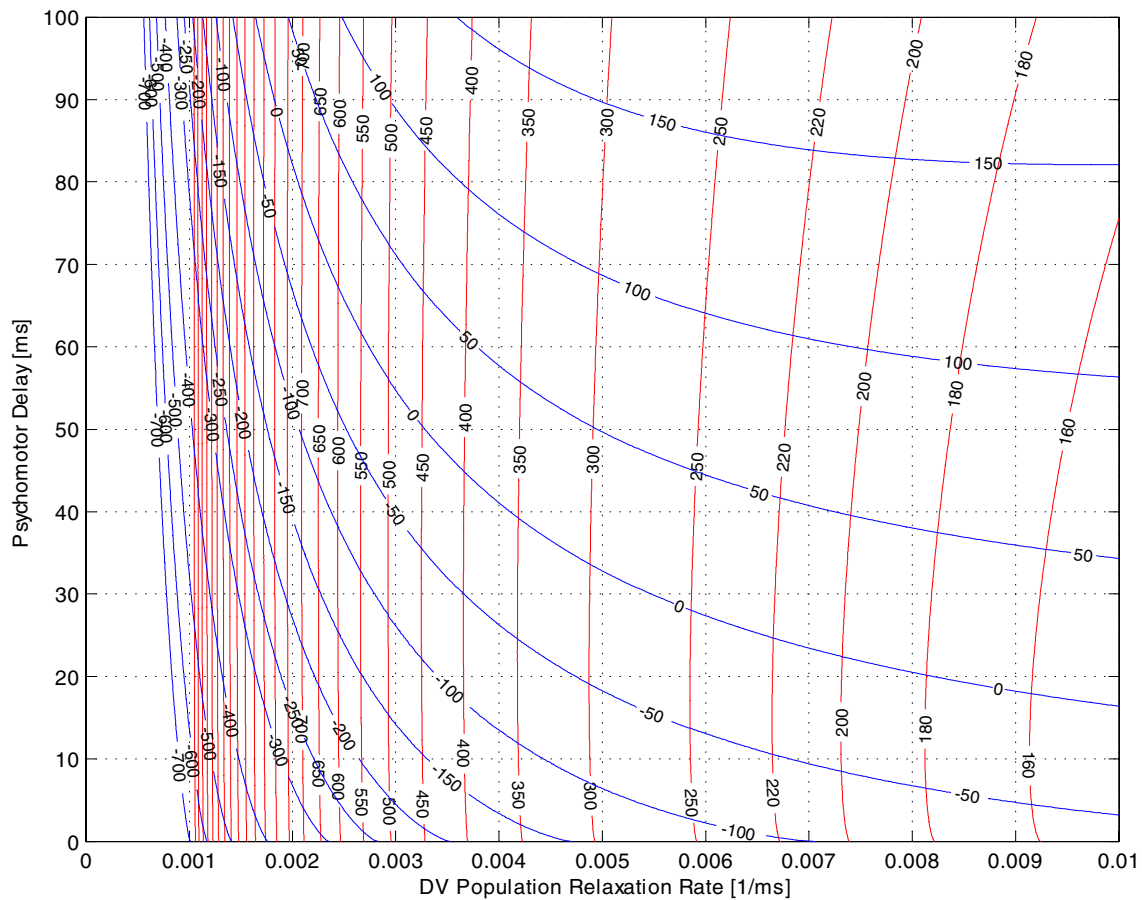
Fig. 7 Contour diagram of the linear regression slope (*red*) and *Y*-intercept (*blue*) dependance on the model parameters using the movement-based definition of movement time. Linear regression was performed at evenly spaced points 0.2 bits apart between 1 and 10 bits (color figure online)

considered were between 0 and 90 ms. The finding of zero delays is not inconsistent with the assumption that nerve conduction delays are present if a forward predictor mechanism exists within the motor circuit.

For the data sets reported in Annett et al. (1958), Glencross and Barrett (1983) Dataset B, and Marteniuk et al. (1987), no delayed feedback model parameters (α, τ) exist, which reproduce the speed–accuracy trade-off reported. This is because the slope and intercept do not satisfy the relationship $-0.482 \leq a/b \leq 3.343$ [bits]. These studies report data having large positive *Y*-intercepts, and a possible explanation is that movement time may be overestimated because "dwell" time or other artifact has been incorporated into the reported value. As mentioned before, the estimated parameters are highly sensitive to errors in the measured movement time data.

4.1 Consideration of effective target width

An important consideration in our analysis of experimental data is the concept of "effective target width" originally

described by Welford (1968). In the classic design of an experiment to measure performance, movement time (the output condition) is determined in response to variation in target width (the input condition). Thus, at the model building stage, the target width W is the independent variable, and MT is the dependent variable. However, as the difficulty of the task diminishes and target width becomes larger, the subject may not take advantage of the entire target area and instead perform the task with a tolerance above that of the experiment design. It is, therefore, important to consider instead the "effective" target width W_e derived by observing the end-point variability when the task is performed. It is the relationship between W_e and movement time that is actually measured.

As discussed in MacKenzie (1991), this adjustment lies at the heart of the information-theoretic metaphor that movements are analogous to "signals" and target width is analogous to noise. The Shannon definition for index of difficulty is based on the premise that the signals are perturbed by white thermal noise so that movement endpoints exhibit a Gaussian spatial distribution. The information in bits (or entropy) of a normal distribution is
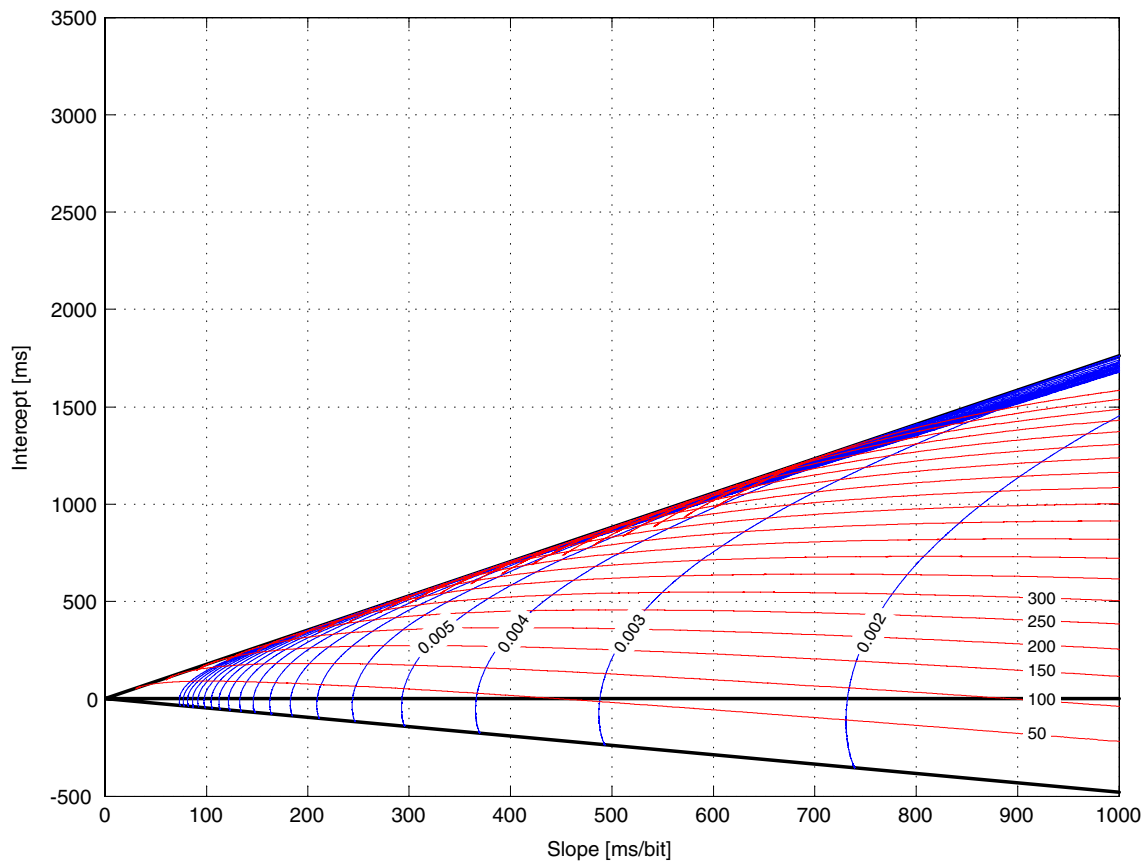
Fig. 8 Contour diagram of the relationship between the linear regression slope and Y-intercept, and the model parameters, delay τ (*red*) and DV population relaxation rate α (*blue*) using the movement-based definition of movement time. Contours for delay are every 50 ms. Contours for relaxation rate are every 0.001 ms/bit. Linear regression was performed at evenly spaced points 0.2 bits apart between 1 and 10 bits (color figure online)

$$H = \log_2\left(\sqrt{2\pi e} \times \sigma\right) = \log_2\left(4.133 \times \sigma\right)$$

where σ is the standard deviation in the unit of measurement. Splitting the constant 4.133 into a pair of z-scores for the unit-normal curve (i.e., $\sigma = 1$), the area bound by $z = \pm 2.066$ represents about 96% of the total area of distribution. In other words, a condition that target width is analogous to the information-theoretic concept of noise is that 96% of the spatial variability lies within the target width while the remaining 4% lie outside or "miss" the target. When an error rate other than 4% are observed, target width should be adjusted to form the effective target width in calculating the ID.

There are two methods for determining the effective target width: the Standard Deviation (SD) or the Discrete Errors (DE) method. If the standard deviation in the endpoint coordinates is known, we just multiply by 4.133 to obtain the effective target width W_e^{SD} that contains 96% of the spatial variability. Alternatively, when the percent of DE is known, we may use a table of z-scores to determine the width W_e^{DE} that would contain 96% of the spatial variability given the actual target width and percent errors. For example, if an experiment with a target width of 5 cm resulted in missing the target 2% of the time, then

$$W_e^{\text{DE}} = \left(\frac{2.006}{z}\right) \times W = \frac{2.006}{2.326} \times 5 = 4.45 \text{ cm}$$

where z is the z-score such that $\pm z$ contains 2% of area under the unit-normal curve.

Figures 13 and 14 contain graphs of the estimated parameters for the computer input data from MacKenzie (1991) adjusted using the SD and DE method, respectively. Using the adjusted data changes the estimate of delay from 0 to 65 ms with the SD method, and from 10 to 110 ms for the DE method. Figure 10 additionally contains estimated parameters for Fitts' reciprocal tapping experiment for which an adjustment for accuracy using the DE method has been done. When this is done, the delay estimate becomes almost zero. One possible explanation for this is that the forward predictor mechanism is completely able to compensate for delay in this case. An alternative explanation is that our model lacks reality.

Table 1 Tables of delayed feedback parameters for the data sets presented in MacKenzie (1991)

Study	Linear regression			Delayed feedback			%Diff.
	Slope [s/bit]	Intercept[s]	Diff.	Alpha [1/ms]	Delay [ms]	Diff.	
MacKenzie Thesis—Appendix B							
Unadjusted data							
Tablet pointing	172.8	81.4	93.66	0.00869	36.7	93.45	−0.2
Tablet dragging	197.6	142.1	149.08	0.00768	55.4	151.69	1.7
Mouse pointing	202.0	−1.7	139.61	0.00749	21.2	145.52	4.2
Mouse dragging	206.7	225.6	147.62	0.00747	79.6	147.71	0.1
Trackball pointing	270.5	197.0	279.57	0.00560	76.0	279.88	0.1
Trackball dragging	331.4	184.4	410.61	0.00456	78.6	414.51	0.9
Adjusted for accuracy (SD)							
Tablet pointing	203.5	−54.8	148.09	0.00750	9.9	149.41	0.9
Tablet dragging	275.6	−27.3	132.18	0.00544	25.3	141.27	6.9
Mouse pointing	222.6	−107.3	154.73	0.00700	3.9	163.13	5.4
Mouse dragging	248.8	134.6	141.69	0.00608	57.9	145.07	2.4
Trackball pointing	299.8	75.3	290.86	0.00503	48.5	293.68	1.0
Trackball dragging	688.4	−348.5	711.39	0.00245	25.7	729.80	2.6
Adjusted for accuracy (DE)							
Tablet pointing	191.4	11.2	127.92	0.00786	21.8	129.60	1.3
Tablet dragging	242.2	77.7	122.10	0.00624	43.5	124.69	2.1
Mouse pointing	218.8	−78.4	160.61	0.00708	9.0	173.18	7.8
Mouse dragging	238.4	184.4	137.68	0.00637	70.0	139.20	1.1
Trackball pointing	296.8	88.1	284.68	0.00506	50.4	286.30	0.6
Trackball dragging	394.2	163.2	358.97	0.00383	79.5	362.42	1.0
Fitts (1954)							
1oz stylus-unadjusted	111.5	27.7	68.59	0.01358	18.4	74.36	8.4
1oz stylus-adjusted (DE)	122.0	−31.4	67.55	0.01253	6.6	75.65	12.0
1lb stylus-unadjusted	123.7	9.7	87.43	0.01236	16.3	96.73	10.6
1lb stylus-adjusted (DE)	142.4	−85.2	71.84	0.01107	0.0	83.24	15.9
Pin transfer	89.4	84.4	240.23	0.01728	31.7	239.47	−0.3
Disc transfer	92.6	223.4	244.67	0.02428	90.4	243.12	−0.6
Andres and Hartung (1989)							
Dataset A	183.7	1.5	110.03	0.00841	21.6	116.32	5.7
Dataset B	173.5	7.6	96.60	0.00881	20.6	97.36	0.8
Dataset T	178.6	4.5	90.96	0.00860	21.1	95.07	4.5
Annett et al. (1958)							
Dataset A	50.0	197.9	35.28	1.11495	88.1	44.03	24.8
Dataset B	49.0	162.3	15.33	1.22683	81.0	18.53	20.8
Dataset C	46.1	197.0	25.65	1.17231	83.6	38.80	51.3
Dataset T	43.0	243.3	98.48	1.12945	88.0	113.97	15.7
Glencross and Barrett (1983)							
Dataset A	94.6	107.8	77.71	0.01644	38.1	78.46	1.0
Dataset B	25.8	183.7	252.35	1.39697	66.9	259.80	3.0
Drury (1975)	102.1	137.5	40.62	0.01545	47.4	41.40	1.9
Gan and Hoffmann (1988)	33.1	99.0	170.65	0.07442	38.1	170.08	−0.3
Kerr (1973)							
Dataset A	94.6	107.8	77.71	0.01644	38.1	78.46210	1.0
Dataset B	154.3	−5.2	72.27	0.00950	10.5	73.81	2.1
Dataset T	136.4	−5.1	41.13	0.01075	9.2	42.17	2.5
Kerr (1977)	63.2	35.1	307.09	0.02358	14.2	307.08	0.0
Kerr (1978)							
Dataset A (land)	118.0	−5.3	46.19	0.01237	7.7	39.43	−14.6
Dataset B (water)	109.9	127.4	231.50	0.01437	46.5	231.82	0.1
Kerr and Langolf (1977)	82.6	−29.9	102.90	0.01815	1.2	106.70	3.7
Kvalseth (1976)	135.8	−15.4	95.58	0.01116	10.8	93.48	−2.2
Kvalseth (1977)	84.9	72.7	71.95	0.01793	26.9	72.02	0.1
Marteniuk et al. (1987)							
Dataset A	53.3	111.3	38.51	0.03270	38.7	38.44	−0.2
Dataset B	64.3	239.8	49.67	0.60908	112.8	49.61	−0.1
Sugden (1980)							
Dataset A	144.9	116.8	59.11	0.01052	44.0	60.37	2.1
Dataset B	80.8	120.7	26.21	0.01952	40.6	26.43	0.8
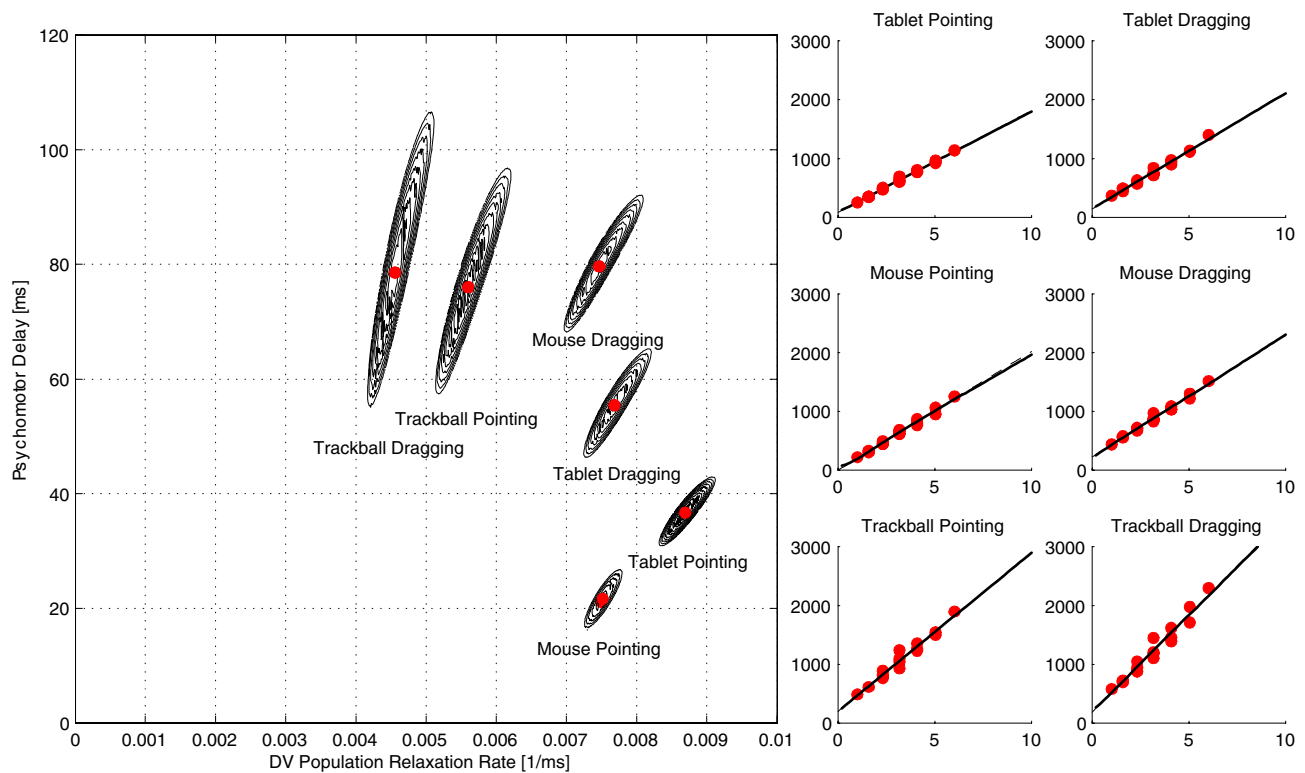
Fig. 9 Estimation of parameters for the motor circuit involved in performing computer input tasks (data from MacKenzie 1991 Appendix B) using unadjusted data. For each task, the point of minimum least square difference with the measured data is indicated in *red* along with contours at every 1% of the least squares difference obtained for the linear regression to a maximum of 10%. For comparison, the measured data, linear regression (*broken line*), and the delayed-feedback performance curve that best matches the data are given (*solid line*). The *X*-axis contains the task ID in bits and the *Y*-axis contains the measured movement time in milliseconds (color figure online)

5 Conclusion

In this article, we have described a relationship between the Fitts' law coefficients and the parameters of a delayed feedback model for human or mechanical motor control. From this, it becomes possible to estimate physiological properties of the motor circuit such as psychomotor delay from measurement of the speed–accuracy trade-off. This method consistently gives an estimate for the effective total motor circuit delay of between 0 and 120 ms for several tasks with performance data that have been reported in the literature. In addition, it is shown that if we assume human movement is generated by the delayed feedback circuit described here, then the Fitts' law coefficients must always satisfy the relationship $-0.482 \leq a/b \leq 3.343$ [bits] where b represents slope (in bits per second) and a the *Y*-intercept in seconds. This is a direct consequence of delay imposing a maximum limit on the performance that can be achieved by linear feedback when only unidirectional movement is possible (Beamish et al. 2008). In fact, we should expect the behavioral properties elaborated here to emerge in *any* delayed linear feedback control that is only capable of unidirectional movement. Figure 15 shows that the data sets considered here

support this conclusion. The few exceptions we attribute to experimental design that systematically overestimates movement times or failure to apply the adjustment for accuracy.

The purpose of this article is not to purport that the delayed VITE model is an accurate description of the physiology underlying motor control, but rather to consider the simplest model necessary to show the emergent properties of delayed feedback described here. In fact, there are several obvious deficiencies in the model. For example, the VITE circuit does not account for the observation of terminal phase submovements that are seen in high ID reciprocal aiming tasks (Meyer et al. 1988). Although there is no widely accepted model for this, correction of the terminal phase likely involves auxiliary motor circuits that come online, as visual, proprioceptive, or forward predictor information become available to correct for neuromuscular noise and inaccuracy of the initial control plan. This explains why submovement corrections generally occur when movement times are larger.

Another obvious deficiency is that the noiseless and deterministic circuit discussed here does not consider the effect of uncontrolled random perturbations in nerve and muscle activity that presumably gives rise to the spatiotemporal variability of normal movements. In fact, recent study in this
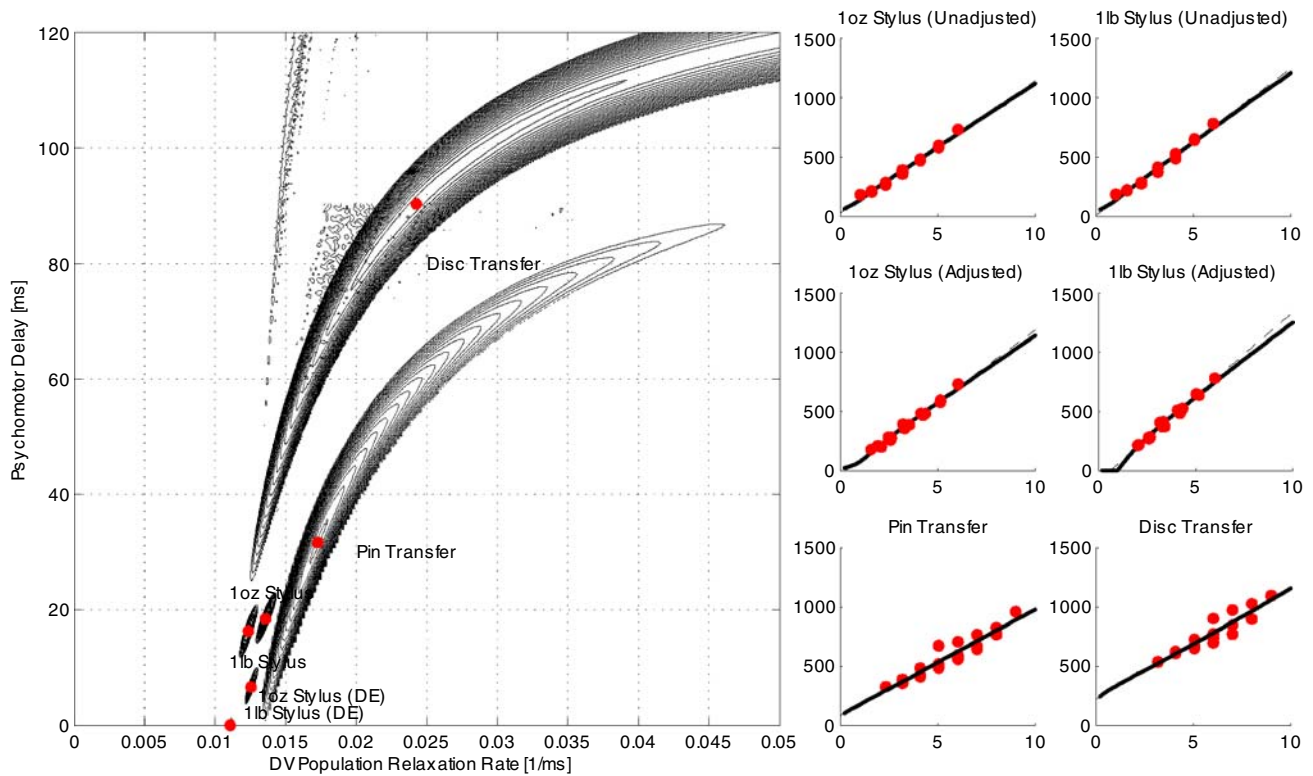
Fig. 10 Estimation of parameters for the motor circuit involved in performing Fitts reciprocal tapping with 1oz and 1lb stylus (using unadjusted and discrete error-adjusted data), pin, and disc transfer tasks. For each task, the point of minimum least square difference with the measured data is indicated in *red* along with contours at every 1% of the least squares difference obtained for the linear regression to a maximum of 20%. For comparison, the measured data, linear regression (*broken line*), and the delayed-feedback performance curve that best matches the data are given (*solid line*). The *X*-axis contains the task ID in bits, and the *Y*-axis contains the measured movement time in milliseconds (color figure online)

area has shown that the presence of noise can statistically stabilize circuits that are tuned near the edge of instability and may, therefore, be an important aspect of human motor control (Venkadesan et al. 2007; Moreau and Sontag 2003; Cabrera et al. 2004; Cabrera and Milton 2004). Although the deterministic circuit has the advantage of a tractable mathematical analysis, perhaps the proper framework for understanding the neurodynamics of human motor control would be a system of stochastic delay differential equations that includes signal-dependent or other noise terms. The results presented here may hopefully serve as a starting point for such studies.

However, even if our model was completely realistic, the motor circuit parameters we estimate are also sensitive with regard to how we choose to define the movement time of a VITE circuit trajectory. In order to further complicate things, the movement times for a task measured during an experiment may not be entirely attributable to the operation of the VITE circuit. Dwell time and terminal phase submovements generated by auxiliary circuits not described by the model may obfuscate the true values of MT required to make a reliable estimate. The estimate is also highly sensitive to whether

adjustment for accuracy is used to account for subjects not taking advantage of the entire target area during a task.

Delay within the motor circuit potentially arises from many sources such as sensory transduction, latencies in central processing, and in motor output. Many studies have quantified the synaptic delay between two single neurons and an approximate value is 1–2 ms (Carr and Konishi 1988; Sabatini and Reghr 1996; Stratford et al. 1996). The delay associated with conduction along the axon depends on the length of the axon and whether the axon is myelinated or nonmyelinated, with values determined to be between 1 and 20 ms (Macefield and Gandevia 1992; Burke et al. 1994). Actual motor circuit delays are difficult to measure, and values have been reported from about 30 ms for a spinal reflex up to 300 ms for a visually guided response, and have additionally been found to be dependent on task demands (Keele and Posner 1968; Zelaznik et al. 1983; Barrett and Glencross 1989; Miall 1996). For a discussion, see Wu (2001).

The delay estimates given here are frequently smaller than the minimum delay that would be required for motor control to be based on afferent proprioceptive feedback or visual guidance unless an internal forward model operates to

Fig. 11 A plot of the estimated delays and time constants for the data sets from MacKenzie (1991). Omitted are the data sets from Annett et al. (1958) (data sets A,B,C,T), Glencross and Barrett (1983) (data set B), and Marteniuk et al. (1987) (data set B) for which the nonlinear regression does not reach a satisfactory minimum. Data sets from the three studies for which no delayed feedback parameters exist corresponding to the observed speed–accuracy trade-off have been omitted
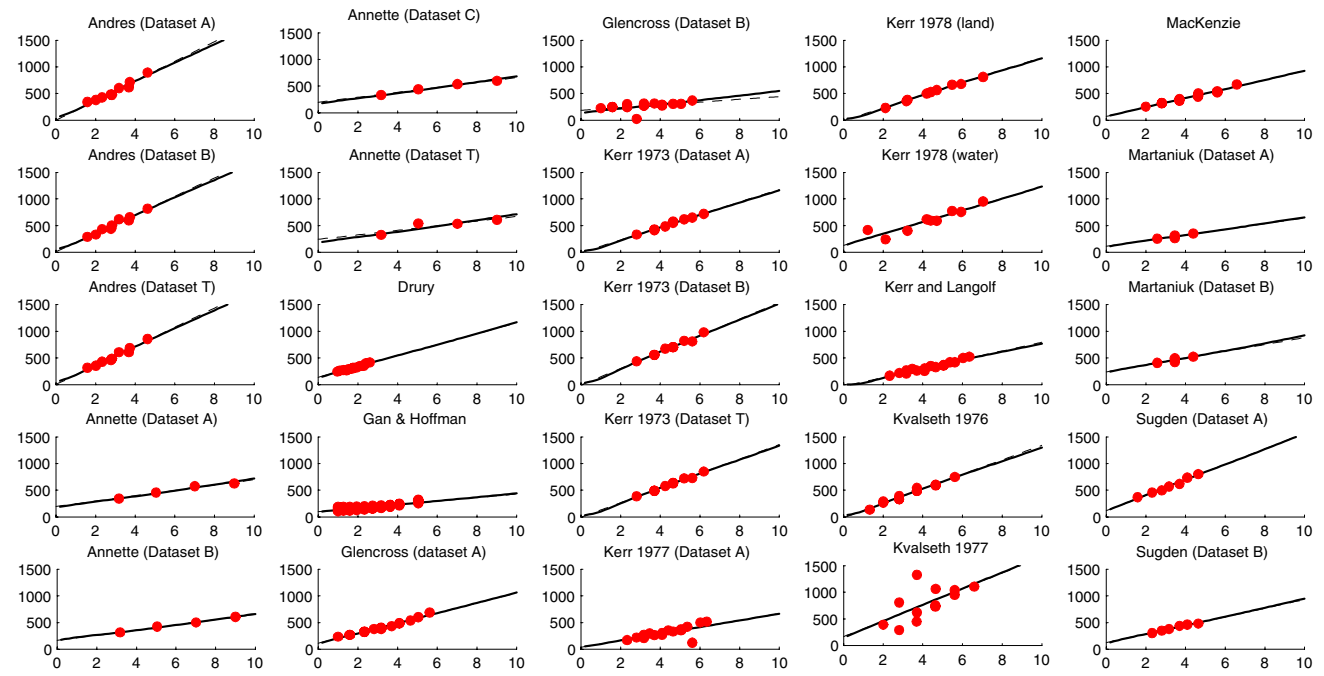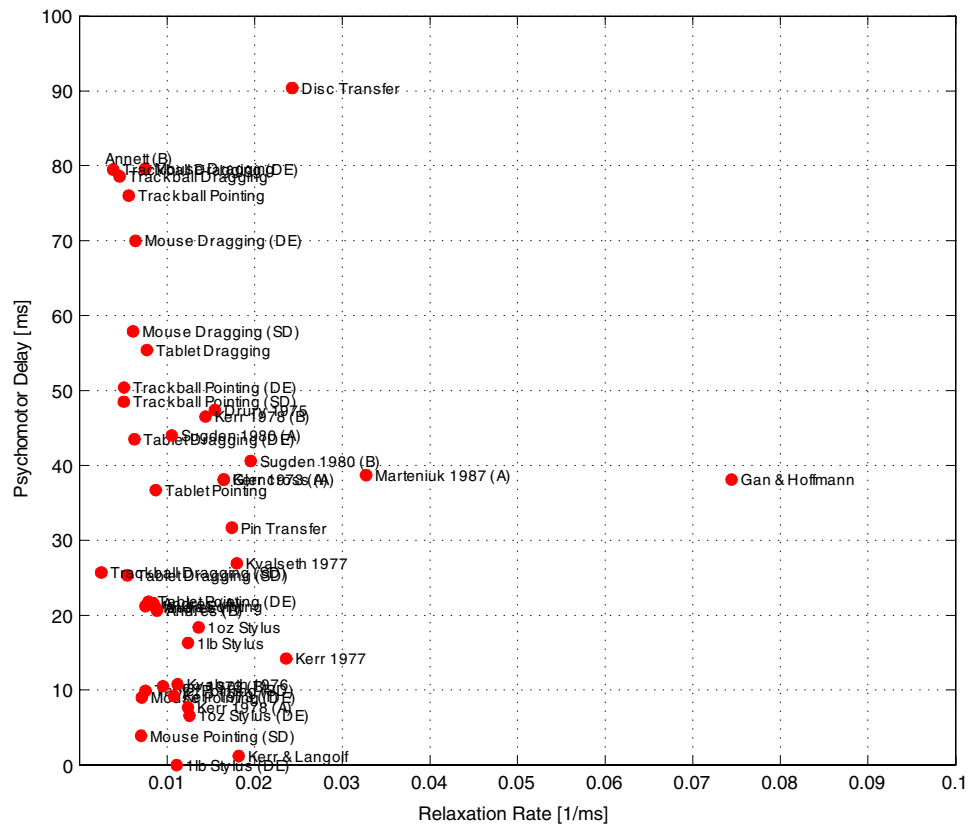
Fig. 12 Graphs of the remaining data sets from MacKenzie (1992) Appendix A, the linear regression (*broken line*), and the performance of the VITE curve with parameters best fitting the data (*solid line*). The *x*-axis represents ID (in bits), and the *y*-axis represents movement time (in milliseconds). The parameters of best fit corresponding to each graph are given in Fig. 11
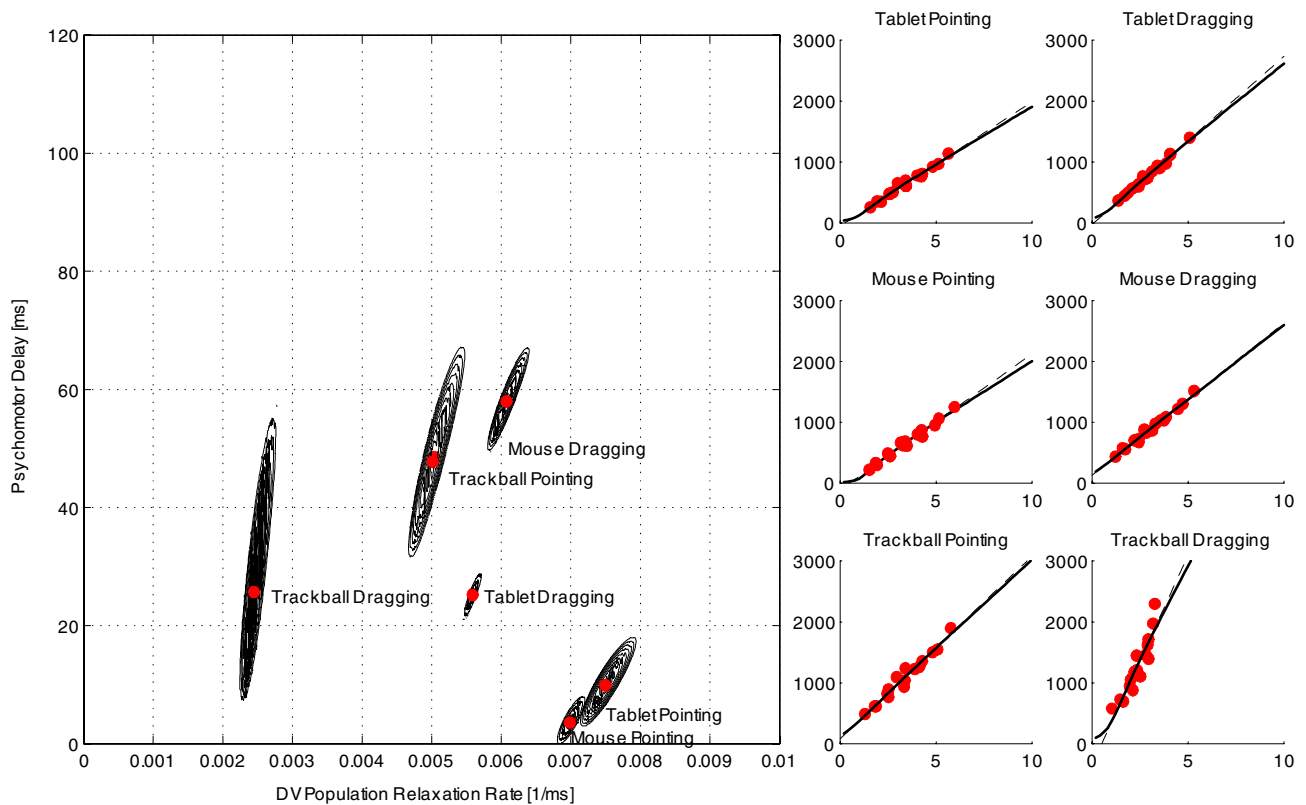
Fig. 13 Estimation of parameters for the motor circuit involved in performing computer input tasks (data from MacKenzie 1991 Appendix B) using standard deviation-adjusted data. For each task, the point of minimum least square difference with the measured data is indicated in *red* along with contours at ev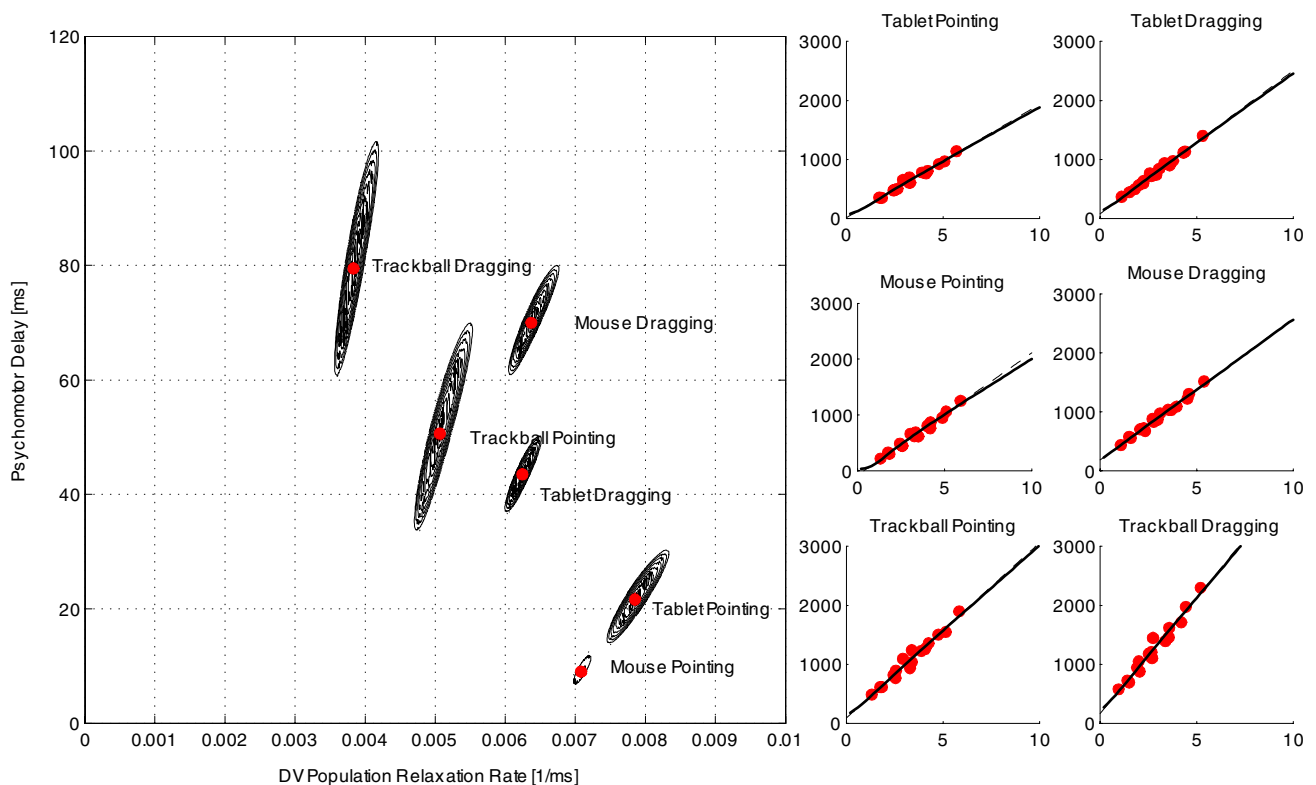ery 1% of the least squares difference obtained for the linear regression to a maximum of 10%. For comparison, the measured data, linear regression (*broken line*), and the delayed-feedback performance curve that best matches the data are given (*solid line*). The *X*-axis contains the task ID in bits, and the *Y*-axis contains the measured movement time in milliseconds (color figure online)

compensate for delay by anticipating the response of the body (and environment) to motor commands. Within the VITE circuit, present position information is identified as being derived from an outflow-command integrator located along the pathway between the pre-central motor cortex and the spinal motor neurons. It is likely that the forward predictive model anticipates motor response based on an efference copy of motor commands, which are then integrated to form present position information. The unavoidable delays in neural processing and conduction time for this mechanism are one type of central delay which may still occur when a forward predictive model operates.

We should expect the neural mechanism of the forward predictor and the degree by which it is able to anticipate the response of the body to outflow motor commands to depend on the particular limb, muscle group, and type of motion involved. This would result in systematic differences in the effective delay between tasks and may partially explain some of the variation of the Fitts' law coefficients between tasks that the information paradigm attributes to differences in motor circuit "throughput". The effective delay

may also be affected by transient changes in the response of the muscle plant to outflow motor commands from fatigue, injury, changes in blood flow, etc.; the health of the central nervous system; and the perceived context of the movement (Vetter and Wolpert 2000).

Desmurget et al. (1999) suggest that the posterior parietal cortex can evaluate the current location of the hand by integrating proprioceptive signals from the somatosensory area and efferent copy signals from the motor region. Their conclusion was based on transcranial magnetic stimulation (TMS) applied over the medial intraparietal sulcus disrupting subjects ability to update control during pointing movements to a target that jumps unpredictably. When stimulation was applied, instead of reaching toward new target positions, the subjects reached to the original target position. In trials with stationary target, stimulation had no effect. This is consistent with the presence of a forward model, which then becomes the only source for guiding movements during TMS disruption (Cisek 2001). Tunik et al. (2005) have also recently shown that updating to perturbed grasping trials is blocked with parietal TMS, where DV and PPC information

Fig. 14 Estimation of parameters for the motor circuit involved in performing computer input tasks (data from MacKenzie 1991 Appendix B) using discrete error-adjusted data. For each task, the point of minimum least square difference with the measured data is indicated in *red* along with contours at every 1% of the least squares difference obtained for the linear regression to a maximum of 10%. For comparison, the measured data, linear regression (*broken line*), and the delayed-feedback performance curve that best matches the data are given (*solid line*). The *X*-axis contains the task ID in bits and the *Y*-axis contains the measured movement time in milliseconds (color figure online)

is speculated to be calculated, and that this calculation occurs within 60 ms. This is consistent with the delay estimates presented here.

Winstein et al. (1997) report PET scan measurements of changes in regional cerebral blood flow (rCBF) with ID during a Fitts' paradigm reciprocal tapping task with the right hand. As aiming task difficulty increased, rCBF increased in areas associated with the planning of more complex movements requiring greater visuomotor processing. These included bilateral occipital, left inferior parietal, and left dorsal cingulate cortices–caudal supplementary motor area proper and right dorsal premotor area. As task ID decreased, significant increases in rCBF were evident in the right anterior cerebellum, left middle occipital gyrus, and right ventral premotor area. These areas are associated with aiiming conditions in which the motor execution demands are high and precise trajectory planing is minimal.

In addition, a functional dissociation was reported between larger amplitude aiming conditions (limb transport) versus smaller amplitude type (endpoint targeting) having equal difficulty. Areas with significantly greater rCBF for targeting were the left motor cortex, left dorsal parietal area (left intraparietal sulcus), and left caudate. The areas associated with limb transport included the bilateral occipital lingual gyri and the right anterior cerebellum. This interpretation is consistent with primary motor cortex cells reflecting directional load-independent population coding or the effects of visual signals guiding the movement (Georgopoulos et al. 1986; Georgopoulos 1995) so that when more precise targeting is required motor cortex neurons are recruited to define the trajectory. This finding, therefore, supports the VITE model which identifies the precentral motor cortex as providing the difference vector command and suggests that where more precise targeting is required the demands for this particular motor cortex cell computation would be greater.

Assuming that the estimation method developed here is not a complete fantasy, it would provide a simple, indirect, and noninvasive way to quantify motor circuit delays. Possibly, this could be developed into a clinical diagnostic tool to assess central and peripheral motor circuit function in the context of a variety of diseases known to affect these circuits (such as, for example, Multiple Sclerosis or Guillan-Barre syndrome). However, even if the model is a

Fig. 15 The Fitts' law coefficients of slope and *Y*-intercepts for the studies reported in the Appendices of MacKenzie (1991). For reference, the corresponding delayed VITE circuit parameters are also shown (*broken lines*). Points lying outside the region having corresponding model parameters are most likely attributable to outdated experimental designs that incorporate "dwell time" into the measurement of movement time and thus overestimate the *Y*-intercept. Unadjusted data set are represented by circles while data adjusted for accuracy are represented by squares (SD method) and triangles (DE method)
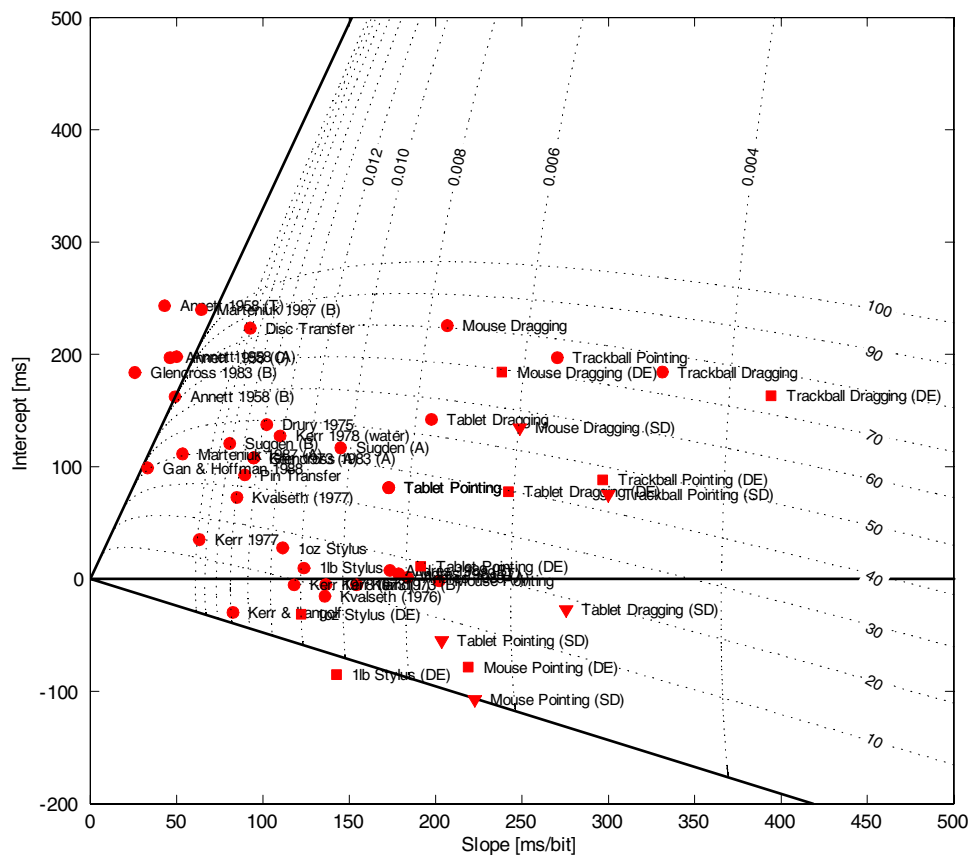
realistic description of the motor circuit, the sensitivity of the estimated effective delay to experiment design might still be a barrier to making accurate estimations. Validation of the delay estimates given here and determining what central neural pathways they might correspond to remain an open question.

References

Andres RO, Hartung KJ (1989) Predictions of head movement time using Fitts' law. Hum Factors 31:703–713

Annett J, Golby CW, Kay H (1958) The measurement of elements in an assembly task: the information output of the human motor system. Q J Exp Psychol 10:1–11

Barrett NC, Glencross DJ (1989) Response amendments during manual aiming movements to double-step targets. Acta Psychol 70: 205–217

Beamish D, Peskun C, Wu J (2005) Critical delay for overshooting in planned arm movements with delayed feedback. J Math Biol 50(1):22–48

Beamish D, MacKenzie IS, Wu J (2006) Speed-accuracy trade-off of planned arm movements with delayed feedback. Neural Netw 19:582–599

Beamish D, Bhatti SA, MacKenzie IS, Wu J (2006) 50 years later: a neurodynamic explanation of Fitts' law. J Royal Soc Interface 3: 649–654

Beamish D, Bhatti S, Wu J, Jing Z (2008) Performance limitations from delay in human and mechanical motor control. Biol Cybern 99: 43–61

Bullock D, Grossberg S (1988) Neural dynamics of planned arm movements: emergent invariants and speed-accuracy properties during trajectory formation. Psychol Rev 95:49–90

Burke D, Gracies JM, Mazevet D, Meunier S, Pierrot-Deseilligny E (1994) Non-monosynaptic transmission of the cortical command for voluntary movement in man. J Physiol 480:191–202

Cabrera JL, Milton JG (2004) Human stick balancing: tuning Levy flights to improve balance control. Chaos 14:691–698

Cabrera JK, Borman R, Eurich C, Ohira T, Milton JG (2004) State-dependent noise and human balance control. Fluct Noise Lett 4:L107–L117

Cannon DJ (1994) Experiments with a target-threshold control theory model for deriving Fitts' law parameters for human-machine systems. IEEE Trans Syst Man Cybern 24(8):1089–1098

Carr CE, Konishi M (1988) Axonal delay lines for time measurement in the owl's brainstem. Proc Natl Acad Sci USA 85:831–8315

Cisek P (2001) A computational perspective on proprioception and movement guidance in parietal cortex. In: Nelson R (ed) The somatosensory system: deciphering the brain's own body image. CRC Press, Boca Raton, FL pp 275–297

Connelly EM (1984) A control model: an alternative interpretation of Fitts' law. In: Proceedings of the 28th Annual Meeting of the Human Factors Society, San Antonio, TX

Desmurget M, Epstein CM, Turner RS, Prablanc C, Alexander GE, Grafton ST (1999) Role of the posterior parietal cortex in updating reaching movements to a visual target. Nat Neurosci 2:563

Drury CG (1975) Application of Fitts' law to foot-pedal design. Hum Factors 17:368–373

Fitts PM (1954) The information capacity of the human motor system in controlling the amplitude of movement. J Exp Psychol 47: 381–391

Fitts PM (1964) The information capacity of discrete motor responses. J Exp Psychol 67:103–112

Fitts PM, Radford BK (1966) Information capacity of discrete motor responses under different cognitive sets. J Exp Psychol 71(4): 475–482

Gan K-C, Hoffmann ER (1988) Geometrical conditions for ballistic and visually controlled movements. Ergonomics 31:829–839

Gawthrop P, Lakie M, Loram I (2007) Predictive feedback control and Fitts' law. Biol Cybern 98:229–238

Georgopoulos AP (1995) Current issues in directional motor control. Trends Neurosci 18:506–510

Georgopoulos AP, Schwartz AB, Kettner RE (1986) Neuronal population coding of movement direction. Science 233:1416–1419

Glencross D, Barrett N (1983) Programming precision in repetitive tapping. J Mot Behav 15:191–200

Hollerback JM, Moore SP, Atkeson CG (1986) Workspace effect in arm movement kinematics derived from joint interpolation. In: Gantchev G, Dimitrov G, Gatev P (eds) Motor control. Plenum Press, New York pp 197–208

Jagacinski RJ, Flach JM (2003) Control theory for humans: quantitative apporaches to modelling performance. Lawrence Erlbaum Associates, Hillsdale

Keele SW, Posner MI (1968) Processing of visual feedback in rapid movements. J Exp Psychol 77:155–158

Kerr BA (1977) Motor control in aimed movements. In: Christina RW, Langers DM (eds) Psychology of motor behavior and sport, vol. I. Human Kinetics Publishers, Champaign, IL pp 269–276

Kerr BA, Langolf GD (1977) Speed of aiming movements. Q J Exp Psychol 29:475–481

Kerr R (1973) Movement time in an underwater environment. J Mot Behav 5:175–178

Kerr R (1978) Diving, adaptation, and Fitts' law. J Mot Behav 10: 255–260

Kvalseth TO (1976) Distribution of movement time in a target-aiming task. Percept Mot Ski 43:507–513

Kvalseth TO (1977) A generalized model of temporal motor control subject to movement constraints. Ergonomics 20:41–50

Macefield G, Gandevia S (1992) Peripheral and central delays in the cortical projections from the human truncal muscles. Brain 115:123–135

MacKenzie IS (1989) A note on the information-theoretic basis for Fitts' law. J Mot Behav 21:323–330

MacKenzie IS (1991) Fitts law as a performance model in human-computer interaction. Doctoral dissertation, University of Toronto

MacKenzie IS (1992) Fitts' law as a research and design tool in human–computer interaction. Hum Comput Interact 7:91–139

MacKenzie CL, Marteniuk RG, Dugas C, Liske D, Eickmeier B (1987) Three-dimensional movement trajectories in Fitts' task: implications for control. Q J Exp Psychol 39A:629–647

Marteniuk RG, MacKenzie CI, Jeannerod M, Athenes S, Dugas C (1987) Constraints on human arm movement trajectories. Can J Psychol 41:365–378

Meyer DE, Abrams RA, Kornblum S, Wright CE, Smith JEK (1988) Optimality in human motor performance: ideal control of rapid aimed movements. Psychol Rev 95(3):340–370

Miall RC (1996) Task dependent changes in visual feedback control: a frequency analysis of human manual tracking. J Mot Behav 28(2):125–135

Miall RC, Wolpert DM (1996) Forward models for physiological motor control. Neural Netw 9:1265–1279

Moreau L, Sontag E (2003) Balancing at the edge of stability. Phys Rev Lett 68:020901

Phillips CA, Repperger DW (1997) Why engineers should know and use Fitts' law? In: Proceedings of the annual international conference of the IEEE engineering in medicine and biology, vol 4. Wright State University, Dayton, pp 1686–1689

Sabatini BL, Reghr WG (1996) Timing of neurotransmission at fast synapses in the mammalian brain. Nature 384:170–172

Soukoreff RW, MacKenzie IS (2004) Towards a standard for pointing device evaluation: perspectives on 27 years of Fitts' law research in HCI. Int J Hum Comput Stud 61:751–789

Stratford KJ, Tarczy-Hornoch K, Martin KAC, Bannister NJ, Jack JJB (1996) Excitatory synaptic inputs to spiny stellate cells in cat visual cortex. Nature 382:258–261

Sugden DA (1980) Movement speed in children. J Mot Behav 12: 125–132

Tunik E, Frey SH, Grafton ST (2005) Virtual lesions of the anterior intraparietal area disrupt goal-dependent on-line adjustments of grasp. Nat Neurosci 8:505–511

Venkadesan M, Guckenheimer J, Valero-Cuevas FJ (2007) Manipulating the edge of instability. J Biomech 40(8):1653–1661

Vetter P, Wolpert DM (2000) Context estimation for sensorimotor control. J Neurophysiol 84:1026–1034

Welford AT (1968) Fundamentals of skill. Methuen, London

Winstein CJ, Grafton ST, Pohl PS (1997) Motor task difficulty and brain activity: investigation of goal-directed reciprocal aiming using positron emission tomography. J Neurophysiol 70(3):1581–1594

Woodworth RS (1899) The accuracy of voluntary movement. Psychol Rev 3:1–119 (monograph supplement)

Wu J (2001) Introduction to neural dynamics and signal transmission delay. De Gruyter series in Nonlinear Analysis and Applications, 6. Walter de Gruyter, Berlin

Zelaznik HN, Hawkings B, Kisselburgh L (1983) Rapid visual feedback processing in single aiming movements. J Mot Behav 15:217–236